

Article

Discovery of New 1,4,6-Trisubstituted-1*H*-pyrazolo[3,4-*b*]pyridines with Anti-Tumor Efficacy in Mouse Model of Breast Cancer †

Maria Georgiou ¹, Nikolaos Lougiakis ¹, Roxane Tenta ², Katerina Gioti ², Stavroula Baritaki ³, Lydia-Evangelia Gkaralea ⁴, Elisavet Deligianni ^{3,4}, Panagiotis Marakos ^{1,*}, Nicole Pouli ¹ and Dimitris Stellas ^{4,*}

¹ Division of Pharmaceutical Chemistry, Department of Pharmacy, School of Health Sciences, National and Kapodistrian University of Athens, Panepistimiopolis Zografou, 15771 Athens, Greece

² Department of Nutrition & Dietetics, School of Health Sciences and Education, Harokopio University, 17671 Athens, Greece

³ Laboratory of Experimental Oncology, Division of Surgery, School of Medicine, University of Crete, 71003 Heraklion, Greece

⁴ Institute of Chemical Biology, National Hellenic Research Foundation, 11635 Athens, Greece

* Correspondence: marakos@pharm.uoa.gr (P.M.); dstellas@eie.gr (D.S.)

† This work is dedicated to the memory of Dr. Leroy B. Townsend.

Abstract: Purine analogues are important therapeutic tools due to their affinity to enzymes or receptors that are involved in critical biological processes. In this study, new 1,4,6-trisubstituted pyrazolo[3,4-*b*]pyridines were designed and synthesized, and their cytotoxic potential was been studied. The new derivatives were prepared through suitable arylhydrazines, and upon successive conversion first to aminopyrazoles, they were converted then to 1,6-disubstituted pyrazolo[3,4-*b*]pyridine-4-ones; this served as the starting point for the synthesis of the target compounds. The cytotoxic activity of the derivatives was evaluated against several human and murine cancer cell lines. Substantial structure activity relationships (SARs) could be extracted, mainly concerning the 4-alkylaminoethyl ethers, which showed potent in vitro antiproliferative activity in the low μM level (0.75–4.15 μM) without affecting the proliferation of normal cells. The most potent analogues underwent in vivo evaluation and were found to inhibit tumor growth in vivo in an orthotopic breast cancer mouse model. The novel compounds exhibited no systemic toxicity; they affected only the implanted tumors and did not interfere with the immune system of the animals. Our results revealed a very potent novel compound which could be an ideal lead for the discovery of promising anti-tumor agents, and could also be further explored for combination treatments with immunotherapeutic drugs.

Keywords: purine analogues; pyrazolopyridine; antiproliferative activity; anticancer agent; in vivo; breast cancer



Citation: Georgiou, M.; Lougiakis, N.; Tenta, R.; Gioti, K.; Baritaki, S.; Gkaralea, L.-E.; Deligianni, E.; Marakos, P.; Pouli, N.; Stellas, D. Discovery of New 1,4,6-Trisubstituted-1*H*-pyrazolo[3,4-*b*]pyridines with Anti-Tumor Efficacy in Mouse Model of Breast Cancer. *Pharmaceutics* **2023**, *15*, 787. <https://doi.org/10.3390/pharmaceutics15030787>

Academic Editors: Noelia Duarte and Ana Paula Francisco

Received: 31 January 2023

Revised: 17 February 2023

Accepted: 24 February 2023

Published: 27 February 2023



Copyright: © 2023 by the authors. Licensee MDPI, Basel, Switzerland. This article is an open access article distributed under the terms and conditions of the Creative Commons Attribution (CC BY) license (<https://creativecommons.org/licenses/by/4.0/>).

1. Introduction

Nitrogen containing fused heterocyclic rings that present a structural analogy to adenine are usually considered privileged scaffolds, since they are often found in many biologically active and clinically useful derivatives. Among them, pyrazolopyrimidine and the closely related pyrazolopyridine pharmacophores are present in druggable small molecule entities, marketed drugs, such as Allopurinol, Zaleplon, Sildenafil, Ibrutinib, and compounds such as Etazolate, that undergo clinical evaluation (Figure 1).

Several pyrazolo[3,4-*b*]pyridine-based derivatives that bear diverse substitutions were reported to exhibit potent antiviral [1,2] and antibacterial [3,4] properties; to inhibit important enzymes, such as phosphodiesterase-4 [5], or neutrophil elastase [6]; and to serve as ligands for A1-adenosine [7] or prostaglandin E2 receptor 1 [8]. The anti-cancer potential of this class of compounds is of particular interest as they show antiproliferative activity,

apoptosis induction, and angiogenesis inhibition [9–11], albeit through diverse molecular targets and mechanisms of action, such as targeting tubulin polymerization [12] and protein kinase signal transduction in cancer cells [10,13–15].

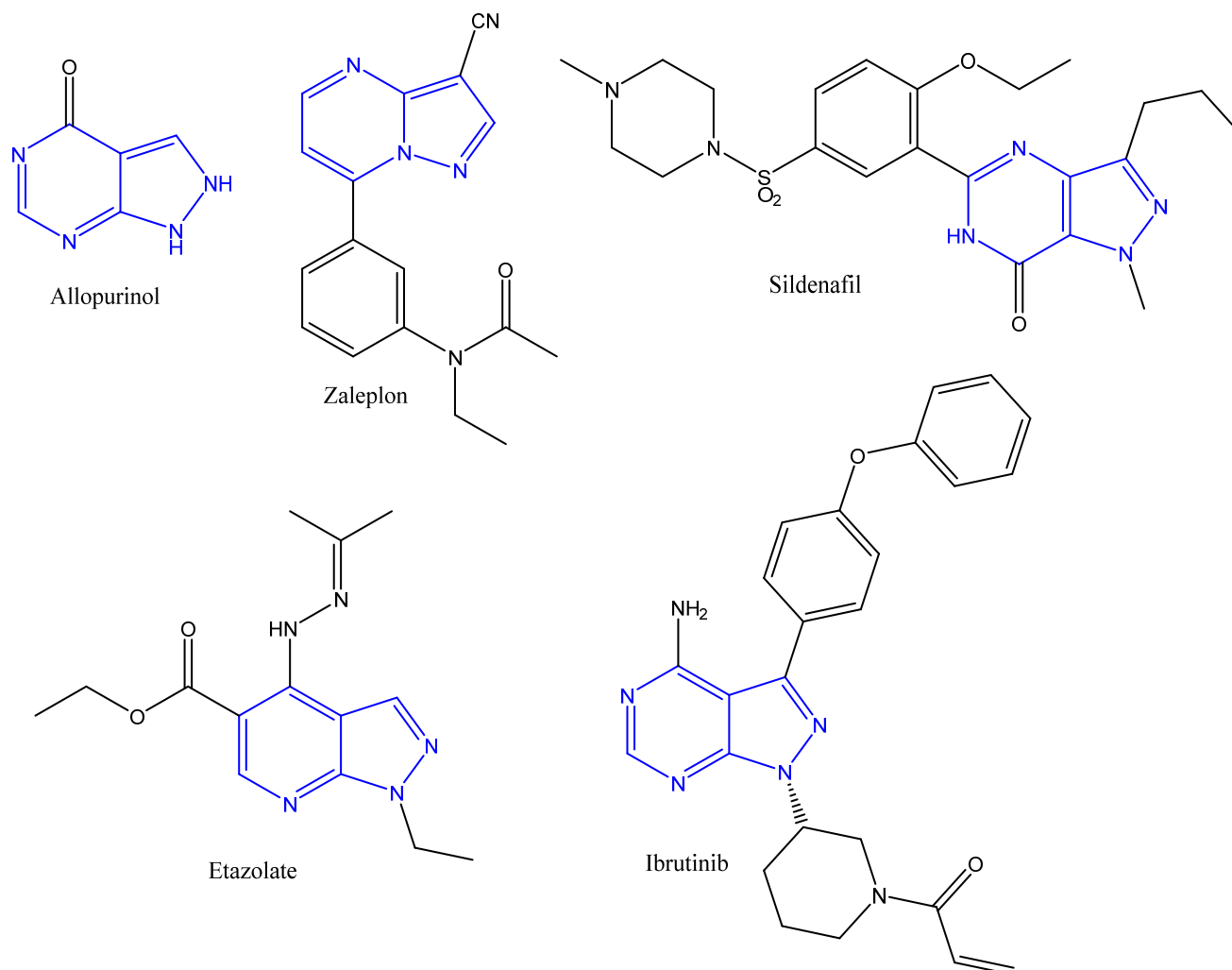


Figure 1. Structures of clinically effective pyrazolopyrimidine and pyrazolopyridine derivatives.

Our long-term aims are the discovery of novel purine analogues with *in vitro* and *in vivo* cytotoxic activity [16,17]. In this respect, we have previously reported on numerous pyrazolo[3,4-*c*]pyridines with potent antiproliferative activity, bearing suitable substituents at critical positions of the central scaffold [18,19]. We observed that the most interesting compounds possessed a 3-aryl group and were also substituted at positions 5 and/or 7 of the original pyrazolo[3,4-*c*]pyridine nucleus. As a continuation of this effort we have designed, synthesized, and evaluated the cytotoxic activity of a new series of compounds which bear the pyrazolo[3,4-*b*]pyridine ring system as their central core. Based on our earlier findings, we have inserted a variety of substituents in specific sites of this scaffold, taking care to preserve the above mentioned substitution pattern, in order to investigate whether the new structural analogues maintain the cytotoxic activity, thereby assisting in the extraction of helpful structure activity relationships. We have also evaluated the efficacy of our newly synthesized analogues *in vitro*, and the three most promising among the new compounds were subsequently evaluated in an orthotopic syngeneic mouse model of breast cancer, prompted by our *in vitro* results.

2. Materials and Methods

2.1. Synthetic Procedures and Analytical Data

Melting points were determined on a Büchi apparatus and are uncorrected. ^1H NMR spectra and 2D spectra were recorded on a Bruker Avance III 600 or a Bruker Avance DRX 400 instrument, whereas ^{13}C NMR spectra were recorded on a Bruker Avance III 600 spectrometer in deuterated solvents and were referenced to TMS (δ scale). The signals of ^1H and ^{13}C spectra were unambiguously assigned by using 2D NMR techniques: $^1\text{H}^1\text{H}$ COSY, NOESY, HMQC, and HMBC. Mass spectra were recorded with a LTQ Orbitrap Discovery instrument, possessing an Ionmax ionization source. The purity of the key compounds (>95%) was determined on a Thermo Finnigan[®] HPLC System (P4000 Pump, AS3000 Autosampler, UV Spectra System UV6000LP detector, Chromquest[™] 4.1 Software); Fortis[®] UniverSil HS-C18 (150 mm, 4.6 mm, 5 μm); mobile phase 1% acetic acid in water/acetonitrile; flow rate 1 mL/min; column temperature 25 $^\circ\text{C}$; injection volume 10 μL ; absorbance at 254 nm). Flash chromatography was performed on Silicagel ACROS ORGANICS 40–60 μm and 60–200 μm , 60A. Analytical thin layer chromatography (TLC) was carried out on precoated (0.25 mm) Merck silica gel F-254 plates.

2,2-Dimethyl-5-((methylthio)[(1-phenyl-1H-pyrazol-5-yl)amino]methylene)-1,3-dioxane-4,6-dione (**5a**)

Dioxanedione **4** (5.55 g, 22 mmol) was added to a solution of the amine **3a** (3.38 g, 21 mmol) [20] in ethanol (50 mL) [20], and the resulting solution was refluxed for 1 h. The solvent was vacuum-evaporated, and the residue was purified by flash column chromatography (silica gel 40–60 μm), and a mixture of cyclohexane/EtOAc (8/2 to 5/5, *v/v*) was used as the eluent, resulting in **5a** (5 g, 78%) as a white solid, mp. 144–146 $^\circ\text{C}$ (Et₂O). ^1H -NMR (600 MHz, CDCl₃) δ (ppm) 1.70 (s, 6H, 2xCH₃), 2.10 (s, 3H, SCH₃), 6.48 (d, 1H, *J* = 1.8 Hz, pyrazole H-4), 7.36–7.41 (m, 1H, phenyl H-4), 7.46–7.49 (m, 4H, phenyl H-2, H-3, H-5, H-6), 7.71 (d, 1H, *J* = 1.8 Hz, pyrazole H-3), 12.52 (brs, 1H, D₂O exch., NH). ^{13}C NMR (151 MHz, CDCl₃) δ (ppm) 18.23, 26.47, 88.57, 103.53, 105.17, 124.25, 128.52, 129.46, 135.34, 138.05, 140.44, 163.67, 179.31. HR-MS (ESI) *m/z* calculated for C₁₇H₁₈N₃O₄S [M+H]⁺: 358.0867; found 358.0846.

2,2-Dimethyl-5-(((methylthio)(1-(3-fluorophenyl)-1H-pyrazol-5-yl)amino)methylene)-1,3-dioxane-4,6-dione (**5b**)

This derivative was prepared by a method analogous to that described for the synthesis of **5a**. Chromatographic purification (silica gel 40–60 μm) was performed by using a mixture of cyclohexane/EtOAc (8/2 to 5/5, *v/v*) as the eluent. Yield: 65%. White solid, mp. 153–155 $^\circ\text{C}$ (CH₂Cl₂/*n*-pentane). ^1H -NMR (600 MHz, CDCl₃) δ (ppm) 1.72 (s, 6H, 2xCH₃), 2.14 (s, 3H, SCH₃), 6.48 (d, 1H, *J* = 2.0 Hz, pyrazole H-4), 7.09 (m, 1H, 3-fluorophenyl H-4), 7.22–7.29 (m, 2H, 3-fluorophenyl H-2, H-6), 7.42 (m, 1H, 3-fluorophenyl H-5), 7.71 (d, 1H, *J* = 2.0 Hz, pyrazole H-3), 12.50 (brs, 1H, D₂O exch., NH). ^{13}C NMR (151 MHz, CDCl₃) δ (ppm) 18.35, 26.49, 88.76, 103.72, 105.85, 111.53, 111.70, 115.34, 115.48, 119.42, 119.43, 130.78, 130.84, 135.40, 139.40, 139.46, 140.87, 162.09, 163.74, 165.69, 179.40. HR-MS (ESI) *m/z* calculated for C₁₇H₁₅FN₃O₄S [M-H][−]: 376.0772; found 376.0763.

2,2-Dimethyl-5-(((1-phenyl-1H-pyrazol-5-ylamino)(phenylamino)methylene)-1,3-dioxane-4,6-dione (**6a**)

Aniline (0.41 mL, 4.5 mmol) was added to a suspension of the methylthio derivative **5a** (1.5 g, 4.18 mmol) in ethanol (17 mL), and the mixture was refluxed for 3 h. The solvent was vacuum-evaporated, and the residue was purified by flash column chromatography (silica gel 40–60 μm), and a mixture of cyclohexane/EtOAc (9/1 to 7/3, *v/v*) was used as the eluent, resulting in **6a** (1.1 g, 65 %) as a foam. ^1H NMR (600 MHz, CDCl₃) δ (ppm) 1.74 (s, 6H, 2xCH₃), 5.77 (d, 1H, *J* = 1.7 Hz, pyrazole H-4), 6.77 (d, 2H, *J* = 7.5 Hz, aniline H-2, H-6), 7.09–7.16 (m, 4H, pyrazole H-3, aniline H-3, H-4, H-5), 7.36–7.52 (m, 5H, phenyl H-2, H-3, H-4, H-5, H-6), 11.63 (brs, D₂O exch., 1H, NH), 12.08 (brs, D₂O exch., 1H, NH). ^{13}C NMR (151 MHz, CDCl₃) δ (ppm) 26.46, 27.03, 75.37, 103.43, 104.48, 123.65, 124.30, 127.23, 128.24, 128.88, 129.52, 133.64, 135.24, 138.13, 139.78, 160.55, 166.52, 167.24. HR-MS (ESI) *m/z* calculated for C₂₂H₂₁N₄O₄ [M+H]⁺: 405.1557; found 405.1557.

2,2-Dimethyl-5-[[1-(3-fluorophenyl)-1H-pyrazol-5-ylamino](phenylamino)]methylene]-1,3-dioxane-4,6-dione (**6b**)

This derivative was prepared by a method analogous to that described for the synthesis of **6a**. Chromatographic purification (silica gel 60–200 μm) was performed by using a mixture of cyclohexane/EtOAc (9/1 to 7/3, *v/v*) as the eluent. Yield: 80%. Yellow oil. $^1\text{H-NMR}$ (600 MHz, CDCl_3) δ (ppm) 1.77 (s, 6H, 2x CH_3), 5.81 (d, 1H, $J = 1$ Hz, pyrazole H-4), 6.77 (d, 2H, $J = 7.5$ Hz, aniline H-2, H-6), 7.07–7.22 (m, 6H, 3-fluorophenyl H-2, H-4, aniline H-3, H-4, H-5, pyrazole H-3), 7.27 (m, 1H, 3-fluorophenyl H-6), 7.43 (m, 1H, 3-fluorophenyl H-5), 11.67 (brs, D_2O exch., 1H, NH), 12.10 (brs, D_2O exch., 1H, NH). $^{13}\text{C-NMR}$ (151 MHz, CDCl_3) δ (ppm) 26.44, 75.39, 103.55, 105.08, 110.99, 111.15, 114.98, 115.12, 118.66, 118.67, 124.45, 127.42, 128.92, 130.73, 130.79, 133.84, 135.06, 139.45, 139.52, 140.19, 160.76, 162.15, 163.79, 166.50, 167.30. HR-MS (ESI) m/z calculated for $\text{C}_{22}\text{H}_{20}\text{FN}_4\text{O}_4$ $[\text{M}+\text{H}]^+$: 423.1463; found 423.1463.

1-Phenyl-6-(phenylamino)-1H-pyrazolo[3,4-*b*]pyridin-4-ol (**7a**)

A solution of **6a** (1.5 g, 3.71 mmol) in diphenyl ether (10 mL) was refluxed under argon for 1 h. The reaction mixture was cooled to ambient temperature and purified by flash column chromatography (40–60 silica gel); a mixture of cyclohexane/EtOAc (9/1 to 4.5/5.5, *v/v*) was used as the eluent, resulting in **7a** as a white solid. Yield 85%, mp. 117–120 $^\circ\text{C}$ (Et_2O). $^1\text{H-NMR}$ (600 MHz, CDCl_3) δ (ppm) 5.91 (s, 1H, H-5), 6.87 (brs, 1H, D_2O exch., NH), 6.98 (t, 1H, $J = 7.1$ Hz, phenyl H-4), 7.18–7.21 (m, 3H, phenyl H-3, H-5, aniline H-4), 7.31–7.36 (m, 4H, aniline H-2, H-3, H-5, H-6), 7.94 (d, 2H, $J = 7.8$ Hz, phenyl H-2, H-6), 7.99 (s, 1H, H-3). $^{13}\text{C-NMR}$ (151 MHz, CDCl_3) δ (ppm) 90.37, 104.93, 121.02, 122.07, 123.51, 126.57, 129.15, 129.22, 132.87, 138.87, 139.66, 150.87, 157.31, 161.17. HPLC purity at 254 nm, 98.24%. HR-MS (ESI) m/z calculated for $\text{C}_{18}\text{H}_{15}\text{N}_4\text{O}$ $[\text{M}+\text{H}]^+$: 303.1240; found 303.1242.

1-(3-Fluorophenyl)-6-(phenylamino)-1H-pyrazolo[3,4-*b*]pyridin-4-ol (**7b**)

This derivative was prepared by a method analogous to that described for the synthesis of **7a**. Chromatographic purification (silica gel 60–200 μm) was performed by using a mixture of cyclohexane/EtOAc (10/1 to 1/10, *v/v*) as the eluent. Yield: 85%. mp. 113–115 $^\circ\text{C}$ (EtOAc/*n*-pentane). $^1\text{H-NMR}$ (600 MHz, acetone- d_6) δ (ppm) 6.26 (s, 1H, H-5), 7.01–7.05 (m, 2H, 3-fluorophenyl H-4, aniline H-4), 7.36 (t, 2H, $J = 7.3$ Hz, aniline H-3, H-5), 7.53 (m, 1H, 3-fluorophenyl H-5), 7.79 (d, 2H, $J = 7.0$ Hz, aniline H-2, H-6), 8.10 (s, 1H, H-3), 8.27 (m, 1H, 3-fluorophenyl H-6), 8.39 (m, 1H, 3-fluorophenyl H-2), 10.14 (brs, 1H, D_2O exch., NH). $^{13}\text{C-NMR}$ (151 MHz, acetone- d_6) δ (ppm) 91.68, 105.20, 107.74, 107.92, 112.07, 112.21, 116.35, 120.60, 122.73, 129.52, 131.13, 131.20, 133.36, 142.04, 142.68, 142.75, 153.19, 158.71, 160.13, 162.98, 164.59. HPLC purity at 254 nm, 96.29%. HR-MS (ESI) m/z calculated for $\text{C}_{18}\text{H}_{14}\text{FN}_4\text{O}$ $[\text{M}+\text{H}]^+$: 321.1146; found 321.1153.

4-Benzyloxy-*N*,1-diphenyl-1H-pyrazolo[3,4-*b*]pyridin-6-amine (**8a**)

K_2CO_3 (47 mg, 0.34 mmol) was added to a solution of the pyridinone **7a** (50 mg, 0.17 mmol) in DMF (3.5 mL); the mixture was stirred for 20 min. Then, benzyl bromide (40 μL , 0.34 mmol) was added, and the resulting mixture was heated at 50 $^\circ\text{C}$ for 3 h. It was then poured into ice water, acidified with 9% HCl solution (pH 3–4), and the precipitate was filtered, dried (CaCl_2) and purified by flash column chromatography (silica gel 40–60 μm); CH_2Cl_2 was used as the eluent to provide pure **8a** (50 mg, 65%) as a white solid. Mp. 228–230 $^\circ\text{C}$ (EtOAc). $^1\text{H-NMR}$ (600 MHz, CDCl_3) δ (ppm) 5.22 (s, 2H, benzyloxy CH_2), 6.09 (s, 1H, H-5), 6.68 (brs, 1H, D_2O exch., NH), 7.10 (t, 1H, $J = 7.6$ Hz, aniline H-4), 7.27 (t, 1H, $J = 7.3$ Hz, phenyl H-4), 7.34 (d, 2H, $J = 7.0$ Hz, aniline H-3, H-5), 7.38–7.45 (m, 7H, benzyloxy 5H, aniline H-2, H-6), 7.49 (t, 2H, $J = 7.3$ Hz, phenyl H-3, H-5), 8.07 (s, 1H, H-3), 8.26 (d, 2H, $J = 8.0$ Hz, phenyl H-2, H-6). $^{13}\text{C-NMR}$ (151 MHz, CDCl_3) δ (ppm) 70.48, 87.63, 104.75, 120.90, 121.29, 123.38, 125.74, 127.57, 128.59, 128.94, 128.98, 129.33, 132.38, 135.73, 139.97, 140.18, 151.85, 157.43, 160.83. HPLC purity at 254 nm, 97.89%. HR-MS (ESI) m/z calculated for $\text{C}_{25}\text{H}_{21}\text{N}_4\text{O}$ $[\text{M}+\text{H}]^+$: 393.1710; found 393.1716.

N,1-Diphenyl-4-(isopentyloxy)-1H-pyrazolo[3,4-*b*]pyridin-6-amine (**8b**)

This derivative was prepared by a method analogous to that described for the synthesis of **8a**. Chromatographic purification (silica gel 40–60 μm) was performed by using CH_2Cl_2

as the eluent. Yield: 98%. White solid, mp. 162–164 °C (EtOAc/*n*-pentane). ¹H-NMR (600 MHz, CDCl₃) δ (ppm) 1.00 (d, 6H, *J* = 6.7 Hz, isopentyl (CH₃)₂CH), 1.77 (m, 2H, isopentyl CH₂CH₂O), 1.88 (m, 1H, isopentyl -CH), 4.13 (m, 2H, isopentyl CH₂O), 6.02 (s, 1H, H-5), 6.73 (brs, 1H, D₂O exch., NH), 7.09 (t, 1H, *J* = 7.3 Hz, aniline H-4), 7.27 (t, 1H, *J* = 7.3 Hz, phenyl H-4), 7.36 (t, 2H, *J* = 7.3 Hz, aniline H-3, H-5), 7.49 (t, 2H, *J* = 7.3 Hz, phenyl H-3, H-5), 7.54 (d, 2H, *J* = 7.0 Hz, aniline H-2, H-6), 8.03 (s, 1H, H-3), 8.28 (d, 2H, *J* = 7.0 Hz, phenyl H-2, H-6). ¹³C NMR (151 MHz, CDCl₃) δ (ppm) 22.66, 25.24, 37.65, 67.17, 87.02, 104.73, 120.71, 121.20, 123.15, 125.61, 128.92, 129.24, 132.32, 140.03, 140.37, 151.85, 157.47, 161.26. HPLC purity at 254 nm, 96.54%. HR-MS (ESI) *m/z* calculated for C₂₃H₂₄N₄NaO [M+Na]⁺: 395.1843; found 395.1850.

4-(2-Bromoethoxy)-*N*,1-diphenyl-1*H*-pyrazolo[3,4-*b*]pyridin-6-amine (8c)

This derivative was prepared by a method analogous to that described for the synthesis of **8a**. The reaction was completed after 6 h. Chromatographic purification (silica gel 40–60 μm) was performed by using a mixture of cyclohexane/CH₂Cl₂/THF (5/5/1 to 4/5/2 *v/v*) as the eluent. Yield: 70%. mp. 199–200 °C (EtOAc/*n*-pentane). ¹H-NMR (600 MHz, acetone-*d*₆) δ (ppm) 3.89 (d, 2H, *J* = 7.0 Hz, bromoethyl CH₂CH₂O), 4.60 (d, 2H, *J* = 7.0 Hz, bromoethyl CH₂CH₂O), 6.30 (s, 1H, H-5), 7.02 (t, 1H, *J* = 7.3 Hz, aniline H-4), 7.30 (t, 1H, *J* = 7.3 Hz, phenyl H-4), 7.35 (t, 2H, *J* = 7.3 Hz, aniline H-3, H-5), 7.54 (t, 2H, *J* = 7.3 Hz, phenyl H-3, H-5), 7.85 (d, 2H, *J* = 7.0 Hz, aniline H-2, H-6), 8.02 (s, 1H, H-3), 8.38 (d, 2H, *J* = 7.0 Hz, phenyl H-2, H-6), 8.62 (brs, 1H, D₂O exch., NH). ¹³C NMR (151 MHz, acetone-*d*₆) δ (ppm) 29.89 (overlapping with solvent), 69.24, 89.49, 104.78, 120.32, 121.46, 122.72, 126.24, 129.56, 129.66, 132.57, 141.13, 142.09, 152.61, 158.49, 160.66. HPLC purity at 254 nm, 96.92%. HR-MS (ESI) *m/z* calculated for C₂₀H₁₈BrN₄O [M+H]⁺: 409.0659; found 409.0667.

1-(3-Fluorophenyl)-4-benzyloxy-*N*-phenyl-1*H*-pyrazolo[3,4-*b*]pyridin-6-amine (8d)

This derivative was prepared by a method analogous to that described for the synthesis of **8a**. Chromatographic purification (silica gel 40–60 μm) was performed by using CH₂Cl₂ as the eluent. Yield: 90%. White solid, mp. 198–200 °C (EtOAc). ¹H-NMR (600 MHz, CDCl₃) δ (ppm) 5.23 (s, 2H, benzyloxy CH₂), 6.11 (s, 1H, H-5), 6.67 (brs, 1H, D₂O exch., NH), 6.95 (t, 1H, *J* = 7.4 Hz, 3-fluorophenyl H-4), 7.12 (t, 1H, *J* = 7.3 Hz, aniline H-4), 7.35–7.44 (m, 10H, benzyloxy 5H, aniline H-2, H-3, H-5, H-6, 3-fluorophenyl H-5), 8.06 (s, 1H, H-3), 8.11 (m, 1H, 3-fluorophenyl H-6), 8.20 (m, 1H, 3-fluorophenyl H-2). ¹³C NMR (151 MHz, CDCl₃) δ (ppm) 70.51, 87.77, 104.92, 108.11, 108.29, 112.03, 112.17, 116.09, 121.09, 123.62, 127.58, 128.64, 128.96, 129.39, 130.09, 130.15, 132.82, 135.62, 139.96, 141.41, 141.48, 152.11, 157.60, 160.82, 162.31, 163.93. HPLC purity at 254 nm, 99.02%. HR-MS (ESI) *m/z* calculated for C₂₅H₂₀FN₄O [M+H]⁺: 411.1616; found 411.1615.

1-(3-Fluorophenyl)-4-(isopentyloxy)-*N*-phenyl-1*H*-pyrazolo[3,4-*b*]pyridin-6-amine (8e)

This derivative was prepared by a method analogous to that described for the synthesis of **8a**. Chromatographic purification (silica gel 40–60 μm) was performed by using CH₂Cl₂ as the eluent. Yield: 82%. mp. 165–167 °C (EtOAc/*n*-pentane). ¹H-NMR (600 MHz, CDCl₃) δ (ppm) 1.00 (d, 6H, *J* = 6.6 Hz, isopentyl (CH₃)₂CH), 1.77 (m, 2H, isopentyl CH₂CH₂O), 1.86 (m, 1H, isopentyl CH), 4.15 (t, 2H, *J* = 7.3 Hz, isopentyl CH₂O), 6.03 (s, 1H, H-5), 6.77 (brs, 1H, D₂O exch., NH), 6.96 (m, 1H, 3-fluorophenyl H-4), 7.13 (t, 1H, *J* = 7.3 Hz, aniline H-4), 7.38–7.45 (m, 3H, 3-fluorophenyl H-5, aniline H-3, H-5), 7.52 (d, 2H, *J* = 7.0 Hz, aniline H-2, H-6), 8.01 (s, 1H, H-3), 8.10 (m, 1H, 3-fluorophenyl H-6), 8.19 (m, 1H, 3-fluorophenyl H-2). ¹³C NMR (151 MHz, CDCl₃) δ (ppm) 22.69, 25.26, 37.63, 67.34, 87.04, 104.94, 108.23, 108.41, 112.18, 112.27, 116.19, 121.16, 123.67, 129.39, 130.14, 130.20, 132.88, 139.98, 141.32, 151.76, 157.60, 161.49, 162.32, 163.93. HPLC purity at 254 nm, 98.70%. HR-MS (ESI) *m/z* calculated for C₂₃H₂₄FN₄O [M+H]⁺: 391.1929; found 391.1930.

4-(2-Bromoethoxy)-1-(3-fluorophenyl)-*N*-phenyl-1*H*-pyrazolo[3,4-*b*]pyridin-6-amine (8f)

This derivative was prepared by a method analogous to that described for the synthesis of **8a**. The reaction was completed after 6 h. Chromatographic purification (silica gel 40–60 μm) was performed by using a mixture of cyclohexane/CH₂Cl₂/THF (5/5/1, *v/v*) as the eluent. Yield: 80%. White solid, mp. 153–155 °C (EtOAc/*n*-pentane). ¹H-NMR (600 MHz, acetone-*d*₆) δ (ppm) 3.88 (d, 2H, *J* = 7.0 Hz, bromoethyl CH₂CH₂O), 4.58 (d, 2H,

$J = 7.0$ Hz, bromoethyl $\text{CH}_2\text{CH}_2\text{O}$), 6.29 (s, 1H, H-5), 7.03–7.06 (m, 2H, 3-fluorophenyl H-4, aniline H-4), 7.37 (t, 2H, $J = 7.3$ Hz, aniline H-3, H-5), 7.55 (m, 1H, 3-fluorophenyl H-5), 7.81 (d, 2H, $J = 7.0$ Hz, aniline H-2, H-6), 8.03 (s, 1H, H-3), 8.25 (m, 1H, 3-fluorophenyl H-6), 8.34 (m, 1H, 3-fluorophenyl H-2), 8.69 (brs, 1H, D_2O exch., NH). ^{13}C NMR (151 MHz, acetone- d_6) δ (ppm) 29.70 (overlapping with solvent), 69.24, 89.59, 104.96, 107.89, 108.07, 112.30, 112.44, 116.50, 120.60, 122.99, 129.58, 131.21, 131.27, 133.15, 141.81, 142.52, 142.59, 152.79, 158.64, 160.67, 162.99, 164.60. HPLC purity at 254 nm, 97.23%. HR-MS (ESI) m/z calculated for $\text{C}_{20}\text{H}_{17}\text{BrFN}_4\text{O}$ $[\text{M}+\text{H}]^+$: 427.0564; found 427.0560.

***N*,1-Diphenyl-4-[2-(phenylamino)ethoxy]-1*H*-pyrazolo[3,4-*b*]pyridin-6-amine (9a)**

A solution of the bromide **8c** (40 mg, 0.098 mmol) and aniline (39 μL , 0.43 mmol) in EtOH (10 mL) was refluxed for 10 h. The solvent was vacuum-evaporated, and the residue was purified by flash column chromatography (silica gel 40–60 μm); a mixture of cyclohexane/ CH_2Cl_2 /THF (7/3/1 to 5/5/1, v/v) was used as the eluent, resulting in pure **9a** as an amorphous pale white solid. Yield 98%. ^1H -NMR (600 MHz, $\text{DMSO-}d_6$) δ (ppm) 3.58 (m, 2H, $\text{CH}_2\text{CH}_2\text{O}$), 4.35 (t, 2H, $J = 5.0$ Hz, $\text{CH}_2\text{CH}_2\text{O}$), 5.84 (t, 1H, $J = 5.7$ Hz, D_2O exch., NH-ethoxy), 6.29 (s, 1H, H-5), 6.57 (t, 1H, $J = 7.3$ Hz, phenylaminoethoxy H-4), 6.70 (d, 2H, $J = 8.0$ Hz, phenylaminoethoxy H-2, H-6), 6.98 (t, 1H, $J = 7.3$ Hz, aniline H-4), 7.11 (t, 2H, $J = 7.6$ Hz, phenylaminoethoxy H-3, H-5), 7.30–7.34 (m, 3H, phenyl H-4, aniline H-3, H-5), 7.55 (t, 2H, $J = 7.6$ Hz, phenyl H-3, H-5), 7.79 (d, 2H, $J = 8.0$ Hz, aniline H-2, H-6), 8.08 (s, 1H, H-3), 8.24 (d, 2H, $J = 8.0$ Hz, phenyl H-2, H-6), 9.42 (brs, 1H, D_2O exch., NH-aniline). ^{13}C NMR (151 MHz, $\text{DMSO-}d_6$) δ (ppm) 41.83, 67.35, 88.70, 103.36, 112.23, 116.00, 118.78, 120.24, 121.34, 125.45, 128.58, 128.90, 132.19, 139.43, 140.90, 148.49, 151.06, 157.22, 159.64. HPLC purity at 254 nm, 96.72%. HR-MS (ESI) m/z calculated for $\text{C}_{26}\text{H}_{24}\text{N}_5\text{O}$ $[\text{M}+\text{H}]^+$: 422.1975; found 422.1958.

***N*,1-Diphenyl-4-(2-(4-methylpiperazin-1-yl)ethoxy)-1*H*-pyrazolo[3,4-*b*]pyridin-6-amine (9b)**

A solution of the bromide **8c** (50 mg, 0.12 mmol) and 4-methylpiperazine (109 μL , 0.98 mmol) in DMF (2.5 mL) was stirred at room temperature for 48 h. Upon completion of the reaction, the mixture was poured into cold water, the precipitate was filtered, washed with water, and air-dried. Chromatographic purification (silica gel 40–60 μm) was performed by using a mixture of CH_2Cl_2 /MeOH (100/0.5 to 100/10, v/v) as the eluent. Yield: 65%. White solid, mp. 164–165 $^\circ\text{C}$ (EtOAc/*n*-pentane). ^1H -NMR (600 MHz, CDCl_3) δ (ppm) 2.30 (s, 3H, CH_3), 2.48 (brs, 4H, piperazine H-3, H-5), 2.66 (brs, 4H, piperazine H-2, H-6), 2.90 (t, 2H, $J = 7.4$ Hz, $\text{CH}_2\text{CH}_2\text{O}$), 4.26 (t, 2H, $J = 7.3$ Hz, $\text{CH}_2\text{CH}_2\text{O}$), 6.04 (s, 1H, H-5), 6.68 (brs, 1H, D_2O exch., NH), 7.10 (t, 1H, $J = 7.3$ Hz, aniline H-4), 7.27 (m, 1H, phenyl H-4, overlapping with solvent), 7.36 (t, 2H, $J = 7.3$ Hz, aniline H-3, H-5), 7.47–7.52 (m, 4H, phenyl H-3, H-5, aniline H-2, H-6), 8.01 (s, 1H, H-3), 8.26 (d, 2H, $J = 7.0$ Hz, phenyl H-2, H-6). ^{13}C NMR (151 MHz, CDCl_3) δ (ppm) 46.16, 53.82, 55.23, 56.82, 66.97, 87.05, 104.66, 121.01, 121.27, 123.43, 125.71, 128.97, 129.36, 132.31, 140.01, 140.27, 151.91, 157.56, 160.95. HPLC purity at 254 nm, 97.27%. HR-MS (ESI) m/z calculated for $\text{C}_{25}\text{H}_{29}\text{N}_6\text{O}$ $[\text{M}+\text{H}]^+$: 429.2397; found 429.2400.

4-(2-(Cyclohexylamino)ethoxy)-*N*,1-diphenyl-1*H*-pyrazolo[3,4-*b*]pyridin-6-amine (9c)

This derivative was prepared by a method analogous to that described for the synthesis of **9b**. Chromatographic purification (silica gel 40–60 μm) was performed by using a mixture of CH_2Cl_2 /MeOH (100/0.5 to 100/15, v/v) as the eluent. Yield: 72%. White solid, mp. 143–145 $^\circ\text{C}$ (EtOAc/*n*-pentane). ^1H -NMR (600 MHz, acetone- d_6) δ (ppm) 1.08–1.22 (m, 3H, cyclohexyl H), 1.25–1.32 (m, 2H, cyclohexyl H), 1.58–1.60 (m, 1H, cyclohexyl H), 1.71–1.74 (m, 2H, cyclohexyl H), 1.91–1.93 (m, 2H, cyclohexyl H), 2.53–2.57 (m, 1H, cyclohexyl H), 3.11 (t, 2H, $J = 5.0$ Hz, $\text{CH}_2\text{CH}_2\text{O}$), 4.28 (t, 2H, $J = 5.0$ Hz, $\text{CH}_2\text{CH}_2\text{O}$), 6.29 (s, 1H, H-5), 7.00 (t, 1H, $J = 7.3$ Hz, aniline H-4), 7.30 (t, 1H, $J = 7.3$ Hz, phenyl H-4), 7.35 (t, 2H, $J = 7.3$ Hz, aniline H-3, H-5), 7.54 (t, 2H, $J = 7.3$ Hz, phenyl H-3, H-5), 7.84–7.86 (m, 2H, aniline H-2, H-6), 8.03 (s, 1H, H-3), 8.38 (d, 2H, $J = 7.0$ Hz, phenyl H-2, H-6), 8.64 (brs, 1H, D_2O exch., NH-aniline). ^{13}C NMR (151 MHz, acetone- d_6) δ (ppm) 25.59, 26.99, 34.28, 46.05, 57.21, 69.81, 89.24, 104.98, 120.22, 121.37, 122.56, 126.12, 129.52, 129.63, 132.73, 141.17, 142.18, 152.53,

158.53, 161.42. HPLC purity at 254 nm, 98.65%. HR-MS (ESI) m/z calculated for $C_{26}H_{30}N_5O$ $[M+H]^+$: 428.2445; found 428.2452.

1-(3-Fluorophenyl)-*N*-phenyl-4-(2-(phenylamino)ethoxy)-1*H*-pyrazolo[3,4-*b*]pyridin-6-amine (**9d**)

This derivative was prepared by a method analogous to that described for the synthesis of **9a**. Chromatographic purification (silica gel 40–60 μ m) was performed by using a mixture of cyclohexane/EtOAc/ CH_2Cl_2 (9/1/1 to 7/3/1, $v/v/v$) as the eluent. Yield 73%. White solid, mp. 173–175 °C (EtOAc/*n*-pentane). 1H -NMR (600 MHz, $CDCl_3$) δ (ppm) 3.67 (t, 2H, $J = 5.0$ Hz, CH_2CH_2O), 4.32 (t, 2H, $J = 5.0$ Hz, CH_2CH_2O), 6.02 (s, 1H, H-5), 6.65 (brs, 1H, D_2O exch., NH), 6.70 (d, 2H, $J = 7.5$ Hz, phenylaminoethoxy H-2, H-6), 6.78 (t, 1H, $J = 7.3$ Hz, phenylaminoethoxy H-4), 6.96 (m, 1H, 3-fluorophenyl H-4), 7.13 (t, 1H, $J = 7.3$ Hz, aniline H-4), 7.23 (t, 2H, $J = 7.3$ Hz, phenylaminoethoxy H-3, H-5), 7.37–7.44 (m, 3H, 3-fluorophenyl H-5, aniline H-3, H-5), 7.51 (d, 2H, $J = 7.1$ Hz, aniline H-2, H-6), 8.02 (s, 1H, H-3), 8.10 (m, 1H, 3-fluorophenyl H-6), 8.20 (m, 1H, 3-fluorophenyl H-2). ^{13}C NMR (151 MHz, $CDCl_3$) δ (ppm) 43.11, 67.36, 87.30, 104.66, 108.13, 108.31, 112.09, 112.23, 113.34, 116.10, 118.39, 121.09, 123.67, 129.39, 129.60, 130.11, 130.17, 132.64, 139.95, 141.35, 141.42, 147.59, 152.05, 157.61, 160.85, 162.30, 163.92. HPLC purity at 254 nm, 95.66%. HR-MS (ESI) m/z calculated for $C_{26}H_{23}FN_5O$ $[M+H]^+$: 440.1882; found 440.1881.

1-(3-Fluorophenyl)-4-[2-(4-methylpiperazin-1-yl)ethoxy]-*N*-phenyl-1*H*-pyrazolo[3,4-*b*]pyridin-6-amine (**9e**)

This derivative was prepared by a method analogous to that described for the synthesis of **9b**. Chromatographic purification (silica gel 40–60 μ m) was performed by using a mixture of CH_2Cl_2 /MeOH (100/8 to 100/16, v/v) as the eluent. Yield: 85%. Amorphous solid. 1H -NMR (600 MHz, $DMSO-d_6$) δ (ppm) 2.26 (s, 3H, CH_3), 2.50–2.59 (brs, 8H, piperazine), 2.84 (t, 2H, $J = 5.0$ Hz, CH_2CH_2O), 4.31 (t, 2H, $J = 5.0$ Hz, CH_2CH_2O), 6.31 (s, 1H, H-5), 7.01 (t, 1H, $J = 7.0$ Hz, aniline H-4), 7.13 (m, 1H, 3-fluorophenyl H-4), 7.34 (t, 2H, $J = 7.5$ Hz, aniline H-3, H-5), 7.57 (m, 1H, 3-fluorophenyl H-5), 7.77 (d, 2H, $J = 8.0$ Hz, aniline H-2, H-6), 8.08–8.11 (m, 2H, H-3, 3-fluorophenyl H-6), 8.26 (m, 1H, 3-fluorophenyl H-2), 9.55 (brs, 1H, D_2O exch., NH). ^{13}C NMR (151 MHz, $DMSO-d_6$) δ (ppm) 45.09, 52.40, 54.33, 55.75, 66.42, 88.99, 103.60, 106.69, 106.87, 111.71, 111.84, 115.47, 119.13, 121.66, 128.62, 130.73, 130.79, 132.76, 140.75, 140.87, 140.95, 151.32, 157.43, 159.55, 161.45, 163.06. HPLC purity at 254 nm, 99.58%. HR-MS (ESI) m/z calculated for $C_{25}H_{28}FN_6O$ $[M+H]^+$: 447.2303; found 447.2300.

4-[2-(Cyclohexylamino)ethoxy]-1-(3-fluorophenyl)-*N*-phenyl-1*H*-pyrazolo[3,4-*b*]pyridin-6-amine (**9f**)

This derivative was prepared by a method analogous to that described for the synthesis of **9b**. Chromatographic purification (silica gel 40–60 μ m) was performed by using CH_2Cl_2 /MeOH as the eluent (100/8 to 100/10, v/v). Yield: 85%. White solid, mp. 280–281 °C (EtOH/diethyl ether). 1H -NMR (600 MHz, $DMSO-d_6$) δ (ppm) 1.07–1.16 (m, 3H, cyclohexyl H), 1.20–1.26 (m, 2H, cyclohexyl H), 1.56–1.58 (m, 1H, cyclohexyl H), 1.69–1.71 (m, 2H, cyclohexyl H), 1.88–1.90 (m, 2H, cyclohexyl H), 2.52–2.54 (m, 1H, cyclohexyl H, overlapping with solvent), 3.08 (t, 2H, $J = 5.5$ Hz, CH_2CH_2O), 4.25 (t, 2H, $J = 5.5$ Hz, CH_2CH_2O), 6.29 (s, 1H, H-5), 7.01 (t, 1H, $J = 7.3$ Hz, aniline H-4), 7.13 (m, 1H, 3-fluorophenyl H-4), 7.34 (t, 2H, $J = 7.3$ Hz, aniline H-3, H-5), 7.57 (m, 1H, 3-fluorophenyl H-5), 7.76 (d, 2H, $J = 7.0$ Hz, aniline H-2, H-6), 8.09 (m, 1H, 3-fluorophenyl H-6), 8.15 (s, 1H, H-3), 8.26 (m, 1H, 3-fluorophenyl H-2), 9.51 (brs, 1H, D_2O exch., NH-aniline). ^{13}C NMR (151 MHz, $DMSO-d_6$) δ (ppm) 24.41, 25.73, 32.55, 44.52, 55.97, 68.28, 88.89, 103.62, 106.69, 106.87, 111.71, 111.85, 115.48, 119.18, 121.71, 128.63, 130.74, 130.80, 132.90, 140.74, 140.89, 140.96, 151.35, 157.46, 159.75, 161.46, 163.07. HPLC purity at 254 nm, 99.99%. HR-MS (ESI) m/z calculated for $C_{26}H_{29}FN_5O$ $[M+H]^+$: 446.2351; found 446.2353.

1-Phenyl-6-(phenylamino)-1*H*-pyrazolo[3,4-*b*]pyridine-4-thiol (**10a**)

Lawesson's reagent (448 mg, 1.11 mmol) was added to a solution of the pyridinol **7a** (280 mg, 0.93 mmol) in dioxane (15 mL), and the mixture was refluxed for 10 h. The solvent was then vacuum-evaporated, and the residue was purified by flash column chromatography (silica gel 40–60 μ m). A mixture of CH_2Cl_2 /EtOAc (100/0.5 to 100/40, v/v)

was used as the eluent. Yield: 20%. Yellow solid, mp. 233–234 °C (EtOAc/*n*-pentane). ¹H-NMR (600 MHz, CDCl₃) δ (ppm) 6.79 (s, 1H, H-5), 6.85 (brs, 1H, D₂O exch., NH), 7.01 (t, 1H, *J* = 7.3 Hz, aniline H-4), 7.22 (t, 2H, *J* = 7.0 Hz, aniline H-3, H-5), 7.30 (t, 1H, *J* = 7.3 Hz, phenyl H-4), 7.43 (d, 2H, *J* = 7.0 Hz, aniline H-2, H-6), 7.49 (t, 2H, *J* = 7.0 Hz, phenyl H-3, H-5), 8.10 (s, 1H, H-3), 8.23 (d, 2H, *J* = 7.1 Hz, phenyl H-2, H-6). ¹³C NMR (151 MHz, CDCl₃) δ (ppm) 101.85, 109.38, 120.63, 121.41, 123.63, 126.22, 129.09, 129.19, 132.02, 139.50, 139.54, 141.10, 149.87, 155.56. HPLC purity at 254 nm, 97.49%. HR-MS (ESI) *m/z* calculated for C₁₈H₁₃N₄S [M-H]⁻: 317.0866; found 317.0850.

1-(3-Fluorophenyl)-6-(phenylamino)-1*H*-pyrazolo[3,4-*b*]pyridine-4-thiol (**10b**)

This derivative was prepared by a method analogous to that described for **10a**. Chromatographic purification (silica gel 40–60 μm) was performed by using a mixture of cyclohexane/EtOAc (75/25, *v/v*) as the eluent. Yield: 18%. White solid, mp. 210–211 °C (acetone). ¹H-NMR (600 MHz, acetone-*d*₆) δ (ppm) 7.02 (t, 1H, *J* = 7.3 Hz, aniline H-4), 7.05 (s, 1H, H-5), 7.12 (m, 1H, 3-fluorophenyl H-4), 7.31 (t, 2H, *J* = 7.3 Hz, aniline H-3, H-5), 7.61 (m, 1H, 3-fluorophenyl H-5), 7.73 (d, 2H, *J* = 7.0 Hz, aniline H-2, H-6), 8.24 (m, 1H, 3-fluorophenyl H-6), 8.30–8.32 (m, 2H, H-3, 3-fluorophenyl H-2), 9.02 (brs, 1H, D₂O exch., NH). ¹³C NMR (151 MHz, acetone-*d*₆) δ (ppm) 102.84, 107.21, 107.39, 108.71, 111.91, 112.05, 115.82, 119.69, 122.50, 128.62, 130.48, 130.54, 132.40, 140.12, 140.44, 141.07, 141.15, 149.82, 155.87, 162.01, 163.61. HPLC purity at 254 nm, 96.53%. HR-MS (ESI) *m/z* calculated for C₁₈H₁₃N₄S [M-H]⁻: 335.0772; found 335.0762.

N,1-Diphenyl-1*H*-pyrazolo[3,4-*b*]pyridin-6-amine (**11a**)

Raney-Ni was added to a solution of the thiol **10a** (120 mg, 0.38 mmol) in EtOH (20 mL), and the mixture was refluxed for 4 h. The reaction mixture was filtered through a celite pad and washed with a mixture of CH₂Cl₂/MeOH (100/10, *v/v*). The filtrate was vacuum-evaporated and purified by flash column chromatography (silica gel 40–60 μm); a mixture of cyclohexane/EtOAc (95/5 to 80/20, *v/v*) was used as the eluent, resulting in pure **11a** (33 mg, 20%) as an amorphous solid. ¹H-NMR (600 MHz, CDCl₃) δ (ppm) 6.64 (d, 1H, *J* = 8.0 Hz, H-5), 6.82 (brs, 1H, D₂O exch., NH), 7.12 (t, 1H, *J* = 7.3 Hz, aniline H-4), 7.29 (t, 1H, *J* = 7.3 Hz, phenyl H-4), 7.37 (t, 2H, *J* = 7.3 Hz, aniline H-3, H-5), 7.51 (t, 2H, *J* = 7.3 Hz, phenyl H-3, H-5), 7.60 (d, 2H, *J* = 7.0 Hz, aniline H-2, H-6), 7.84 (d, 1H, *J* = 8.0 Hz, H-4), 8.00 (s, 1H, H-3), 8.30 (d, 2H, *J* = 7.1 Hz, phenyl H-2, H-6). ¹³C NMR (151 MHz, CDCl₃) δ (ppm) 106.73, 111.15, 120.52, 121.14, 123.26, 125.71, 128.99, 129.23, 131.50, 134.32, 139.88, 140.03, 149.85, 155.27. HPLC purity at 254 nm, 95.31%. HR-MS (ESI) *m/z* calculated for C₁₈H₁₅N₄ [M+H]⁺: 287.1291; found 287.1289.

1-(3-Fluorophenyl)-*N*-phenyl-1*H*-pyrazolo[3,4-*b*]pyridin-6-amine (**11b**)

This derivative was prepared by a method analogous to that described for the synthesis of **11a**. Chromatographic purification (silica gel 40–60 μm) was performed by using CHCl₃ as the eluent. Yield: 18%. Amorphous solid. ¹H-NMR (600 MHz, CDCl₃) δ (ppm) 6.60–6.62 (m, 1H, H-5), 6.85 (brs, 1H, D₂O exch., NH) 6.97 (m, 1H, 3-fluorophenyl H-4), 7.13 (t, 1H, *J* = 7.3 Hz, aniline H-4), 7.38–7.45 (m, 3H, aniline H-3, H-5, 3-fluorophenyl H-5), 7.58 (d, 2H, *J* = 8.0 Hz, aniline H-2, H-6), 7.79–7.81 (m, 1H, H-4), 7.97 (s, 1H, H-3), 8.14 (m, 1H, 3-fluorophenyl H-6), 8.25 (m, 1H, 3-fluorophenyl H-2). ¹³C NMR (151 MHz, CDCl₃) δ (ppm) 106.95, 107.93, 108.11, 111.25, 111.98, 112.12, 115.91, 115.93, 120.65, 123.47, 129.24, 130.10, 130.16, 131.52, 134.75, 139.73, 141.22, 141.29, 149.98, 155.34, 162.25, 163.87. HPLC purity at 254 nm, 97.14%. HR-MS (ESI) *m/z* calculated for C₁₈H₁₄FN₄ [M+H]⁺: 305.1197; found 305.1196.

2.2. In Vitro Cytotoxicity (MTT) Assays

The human HCT116 colon cancer cell line and PC-3 prostate cancer cell line were obtained from the American Type Cell Culture (ATCC, Bethesda, MD, USA). HCT116 and PC-3 cell lines were grown at 37 °C in 5% CO₂ using Roswell Park Memorial Institute 1640 medium (RPMI 1640) and Dulbecco's modified Eagle's medium F/12 (DMEM/F-12) containing 10% fetal bovine serum (FBS). MEFs and KPC cells were cultured in a 5% CO₂, with DMEM medium containing 10% fetal bovine serum (FBS), 100 U/mL Penicillin and

100 mg/mL Streptomycin at 37 °C. EO771 cells were purchased from CH3 BioSystems and cultured in complete RPMI 1640 medium supplemented with 10% fetal calf serum, 100 U/mL Penicillin and 100 mg/mL Streptomycin. To test the inhibitory activities of compounds using a cell-based assay, MTT assays were performed for cell viability. Briefly, in 96-well plates, HCT116 cells were plated at a density of 1500 per well, PC-3 cells were plated at a density of 750 per well; KPC and MEFs were plated at a density of 3000 cells per well; and EO771 were seeded at a density of 2500 cells per well. The differences in the initial seeding cell numbers reflect the differences in the doubling time of cells, given that we sought to have wells that were close to but not confluent at the end of the experiment. After 24 h, cells were treated with the indicated compounds in a dose-dependent manner for 72 h and 96 h. Viable cell numbers were determined by tetrazolium conversion to its formazan dye. All the experiments were performed three times, and the tested concentrations in each experiment were evaluated in quadruplicated wells. Mouse embryonic fibroblasts (MEFs) and KPC pancreatic cells (Kras(mut); Pdx Cre) are cell lines derived from our C57/Bl6 mice and the double transgenic mouse pancreatic cancer model, respectively [21–23].

2.3. Mouse Models

All studies were approved by the National Hellenic Research Foundation Animal Care and Use Committee. The study protocol was approved by the local ethics committee (Athens Prefecture Veterinarian Service; (431956/17-05-2022.) Animal care was provided in accordance with the procedures outlined in the “Guide for Care and Use of Laboratory Animals (National Research Council; 1996; National Academy Press; Washington, DC, USA). C57BL/6 female mice were purchased from Jackson Laboratory. Mice at 6–8 weeks of age were randomly assigned to treatment or control groups. As indicated by the performed power analysis (clinical calculator/clincalc.com), 5 mice per group were used in each of the in vivo experiments. We repeated the in vivo experiments three times and found similar results. In the results section, we present our data from one experiment. The EO771 were cultured in complete RPMI 1640 medium supplemented with 10% fetal calf serum, 50 mM 2-mercaptoethanol, 100 U/mL Penicillin, and 100 mg/mL Streptomycin. Murine EO771 (5×10^5) were orthotopically inoculated at the fourth mammary fat pad of 6–8 weeks old mice. The cells were resuspended in PBS. Matrigel (Corning Inc., Corning, NY, USA) was added at 1:3 dilution to facilitate the inoculation process. Matrigel, an extract of basement membrane proteins, was used as a cell carrier medium for cell transplantation studies by forming a 3D gel at 37 °C that facilitated the inoculation. Tumor size was measured using a digital caliper, and tumor volume (mm^3) was calculated by the following equation: $L*W*H*\pi/6$. The mice were monitored on a daily basis for any signs of discomfort and the orthotopic tumors were also monitored routinely for any signs of ulcerations or any other type of wounds. The mice were also weighted once a week. Per our guidelines, any mouse found with an ulcerated wound, 30% weight loss, or visual signs of discomfort (slow reflexes, not walking normally, hunched back, or rough coat) was immediately excluded from the experiment and euthanized. Despite the strict rules, no mice were excluded from our experiments. All the treatments were well tolerated by the mice, showing no signs of toxicity.

2.4. Treatment of EO771 Tumor-Bearing Mice

Treatment was initiated when tumors reached $\sim 20 \text{ mm}^3$. Animals were treated with **9b**, **9c** and **9e** peritumorally by administration of 100 μg of the aforementioned compounds in Matrigel (Corning Inc.), used in 1:4 dilution, every 4 days. The mice were sacrificed when the primary tumor reached a 2 cm diameter, or at any other humane endpoints as listed in the ACUC-approved animal protocol, such as 20% weight loss or acute morbidity.

2.5. Histology and Immunohistochemistry Staining

Tissue samples, including tumors, were fixed in 10% neutral buffered formalin (NBF, Sigma), then routinely processed and paraffin embedded. Tumor and lung sections were

dewaxed and rehydrated, then stained with hematoxylin and eosin (H&E). For immunohistochemistry, sections were antigen-retrieved with the heat-induced or enzymatic method. Peroxidase activity was blocked using 1.5% hydrogen peroxide. Sections were blocked with different blocking protocols, depending on the antibody. Staining was performed using the following anti-mouse antibodies: anti-Ki67 (Cell Signaling, 9449) (1:1000 dilution) and anti-Caspase 3 (Cell Signaling, 9661) (1:800 dilution). A polymer-based detection kit, which consists of horseradish peroxidase-conjugated polymers was used for detection. To determine proliferation indices, Ki67-positive and Ki67-negative cells were counted using ImageJ software (US National Institutes of Health) in 8–10 representative fields of all tumors (on average, ~3000 nuclei were counted per specimen). A similar approach was followed to evaluate the % percentage of apoptotic cells.

2.6. Statistical Analysis

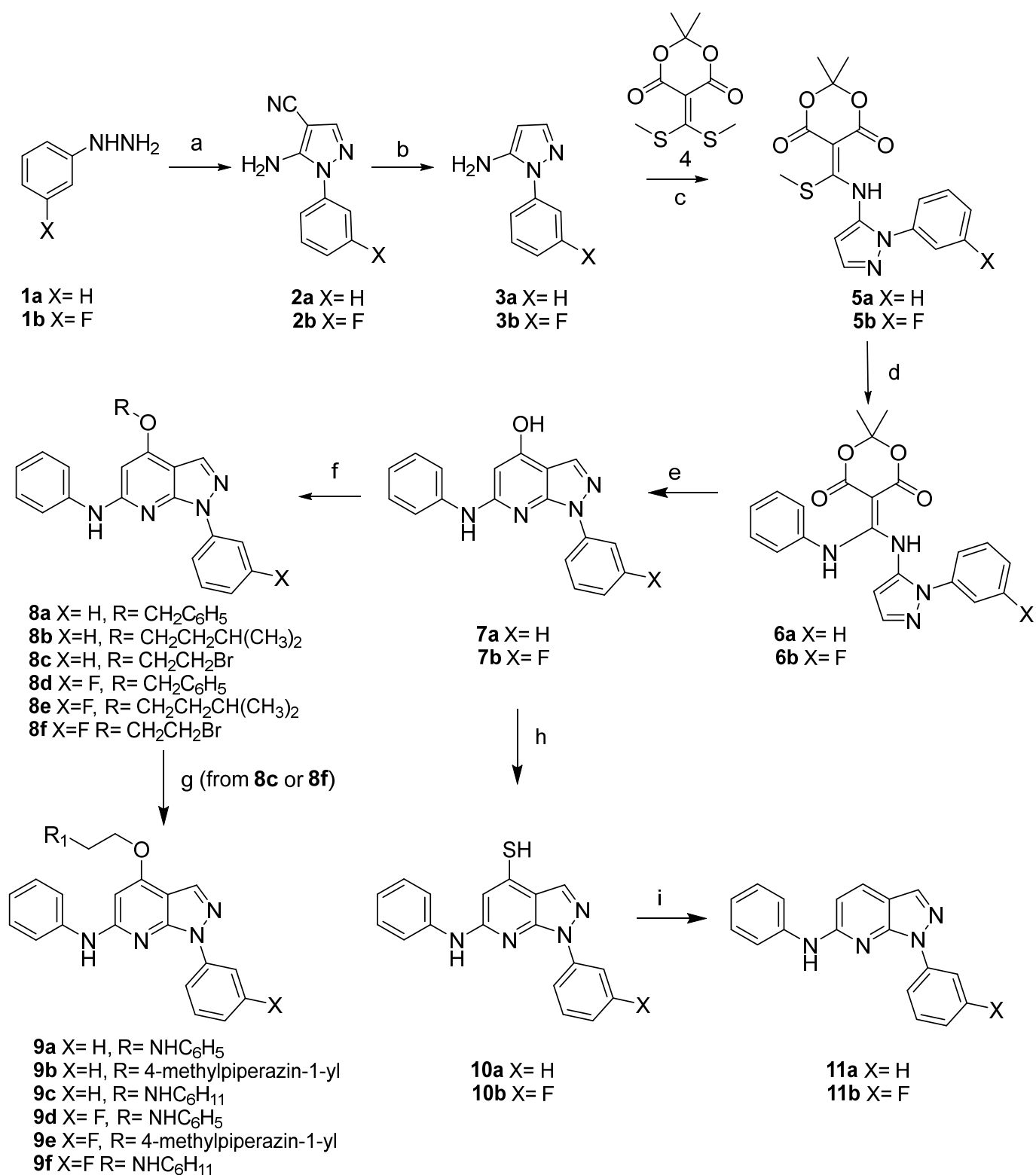
Statistical analyses and graph generation were performed with GraphPad Prism 9.2.0 (San Diego, CA, USA). Tumor areas were plotted as mean \pm standard error of the mean (SEM) for each data point, and tumor growth curves were compared using mixed effects ANOVA. Differences were evaluated by 1-way ANOVA or unpaired parametric Student's *t* test. The *p*-values were calculated for multiple comparisons using Tukey's multiple comparisons test.

3. Results and Discussion

3.1. Synthesis of the Novel Compounds

Upon a literature search for the optimum way to accomplish the synthesis of pyrazolo[3,4-*b*]pyridines [24,25], we have decided to prepare the target compounds by using commercial phenylhydrazine (**1a**) or 3-fluorophenylhydrazine (**1b**) as starting materials (Scheme 1). Each hydrazine was converted to the corresponding pyrazole-4-carbonitriles (**2a,b**) [26,27], and then, upon hydrolysis and subsequent decarboxylation, converted to the pyrazoles **3a,b** following a previously reported methodology [20,28]. The above mentioned pyrazoles were then treated with the Meldrum's acid dimethylthiomethylene-derivative **4** [29] to provide the intermediate dioxanediones **5a,b**. The remaining methylthio group of compounds **5a,b** were then displaced upon reaction with aniline, and the derived dioxanediones **6a,b** were subjected to thermal cyclization and converted to the pyrazolopyridinols **7a,b**.

The pyridinones **7a,b** were treated with K_2CO_3 and suitable bromides to provide the corresponding ethers through their enolates **8a–f**. The unambiguous confirmation for the O-alkylation was evidenced from 2D NMR data. Thus, from the HMBC spectrum, a cross-peak between the most downfield ethoxy side chain methylene with C-4 was obvious, and additionally, data from the nOe spectrum showed that the above-mentioned methylene correlates to both H-5 and H-3 as well. Additionally, the bromides **8c,f** were used for the introduction of selected amines, namely aniline, 4-methylpiperazine, or cyclohexylamine, which resulted in the aminoderivatives **9a–f**. Along with the aim of expanding the structural diversity of this scaffold, compounds **7a,b** were allowed to react with Lawesson's reagent, and the resulting thiols **10a,b** were reduced by using Raney nickel as the catalyst to provide the corresponding 1,6-disubstituted pyrazolopyridines **11a,b**. An alternative pathway for the synthesis of a **7a** modified analogue is also presented in the Supporting Information section in Supplementary Materials (Scheme S1).



Scheme 1. Reagents and conditions. (a) (ethoxymethylene)malononitrile, EtOH abs., reflux, Ar, 80%; (b) H₃PO₄, reflux, 92%; (c) EtOH, reflux, 65–78%; (d) aniline, EtOH, reflux, 65–80%; (e), Ph₂O, reflux, Ar, 85%; (f) (1) K₂CO₃, DMF, (2) RBr, 50 °C, 65–98%; (g) for **9a,9d**: aniline, EtOH, reflux, 73–98%, for **9b,9c,9e,9f**: N-methylpiperazine or cyclohexylamine, DMF, rt, 65–85%; (h) Lawesson's reagent, dioxane, reflux, 20%; (i) Raney Ni, EtOH, reflux, 20%.

3.2. Evaluation of the Antiproliferative Efficacy of the New pyrazolo[3,4-*b*]pyridine Derivatives In Vitro

The cytotoxic activity of all target compounds, **7a,b**, **8a–f**, **9a–f**, **10a,b**, and **11a,b**, was initially evaluated against the prostatic PC-3 and the colon HCT116 human cancer cell lines. This screening provided very interesting information concerning the structural requirements for activity. The majority of the compounds did not exhibit significant activity; they possessed IC₅₀ values greater than 10 μM, with the remarkable exception of two couples of analogously substituted derivatives, specifically, **9b,c** and **9e,f**. The latter were endowed with low μM activity in the IC₅₀ range of 0.75–4.55 μM (Table 1). All four compounds are 4-alkylaminoethoxy derivatives, providing an indication that the presence of a 4-arylaminoether, a 4-arylalkyl or 4-alkyl ether do not encourage activity. This is also true in the case of pyrazolopyridinones **7a,b**, the corresponding thiones **10a,b**, and the 4-unsubstituted analogues **11a,b**. These active analogues were subsequently tested against two additional cancer cell lines and one non-cancerous murine cell line. The first murine cancer cell line, EO771, is a breast cancer cell line, syngeneic to C57/Bl6; the second cell line, KPC, is a pancreas cancer cell line, syngeneic to C57/Bl6. The non-cancerous murine cell line consists of mouse embryonic fibroblasts (MEFs) and is also derived from C57/Bl6 mice.

Table 1. Antiproliferative activities of the most active derivatives.

Compound	IC ₅₀ Values (μM) ^a				
	PC3	HCT116	EO771	KPC	MEFs
9b	4.55 ± 0.50	2.40 ± 0.20	1.50 ± 0.70	16.90 ± 2.50	>200
9c	0.75 ± 0.15	1.05 ± 0.05	1.45 ± 0.30	8.74 ± 0.90	>200
9e	4.15 ± 0.15	3.65 ± 0.25	2.95 ± 0.80	133.2 ± 3.4	>200
9f	1.95 ± 0.05	2.35 ± 0.45	1.95 ± 1.20	17.47 ± 1.60	11.2 ± 1.3
Dox	0.025 ± 0.01	0.095 ± 0.01	0.825 ± 0.30	2.23 ± 0.40	5.4 ± 0.8

^a Results presented are means ± standard deviation (SD) of three independent experiments and are expressed as IC₅₀, i.e., the effective concentration reducing viability by 50% compared to unexposed control cells; Dox: doxorubicin.

Cell viability of the four derivatives against normal mouse embryonic fibroblasts (MEFs) was also examined. Three compounds were found non-toxic (**9b**, **9c** and **9e**, presenting IC₅₀ >200 μM), and the fourth showed severe cytotoxicity with an IC₅₀ = 11.2 μM. Figure 2 depicts the comparison of the IC₅₀ curves of the selected **9b** (Figure 2A), **9c** (Figure 2B), **9e** (Figure 2C), and **9f** (Figure 2D) in mouse embryonic cells and EO771 mouse breast cancer cell. The difference in the cell viability between those cell lines indicate possible anti-breast cancer efficacy of these compounds and minimal off target effects. It is noteworthy that those compounds were not as effective in reducing the cell proliferation of the KPC mouse pancreatic cell line, suggesting possible breast cancer specificity. Based on our in vitro data, we decided to investigate the efficacy of **9b**, **9c**, and **9e** in vivo in our tumor bearing EO771 mouse model. Only **9f** was excluded from the subsequent in vivo experiments because of its low IC₅₀ values on the MEFs, so that potential increased toxicity or lethality to the experimental animals could be avoided.

3.3. Evaluation of the Anti-Cancer Efficacy of the Most Active Analogues In Vivo

We next sought to investigate the efficacy of the novel compounds in mouse syngeneic models of cancer, enabling us to monitor the effects of the treatment not only to the tumor growth itself, but also to the immune system of the mouse, which better simulated the interactions we often monitor in clinical settings. For subsequent in vivo analysis, we chose EO771 cells as they showed very good IC₅₀ values and specificity in comparison to the pancreatic cell line or the non-cancerous fibroblasts. We thus established mouse tumors by using EO771 cells and orthotopically inoculated into the mammary fat pad of the mouse. At 6–7 days after inoculating 5 × 10⁵ cells into the mammary fat pad, the mice develop palpable tumors; immediately after this observation, we initiated our treatment with the

selected compounds. Based on our previous *in vivo* studies [21], and the fact that all the *in vivo* evaluated agents showed minimal toxicity on the mouse embryonic fibroblasts, we initiated a treatment protocol of intraperitoneal delivery of 100 μg every four days until day 26 post-inoculation. As presented in Figure 3, all the tested compounds resulted in a strong inhibition of tumor growth (Figure 3A). The compound-specific tumor growth curves revealed that **9b** was more potent in inhibiting tumor growth in comparison to the other analogues. (Figure 3B–D). The treatment schedule is depicted in Figure 3E.

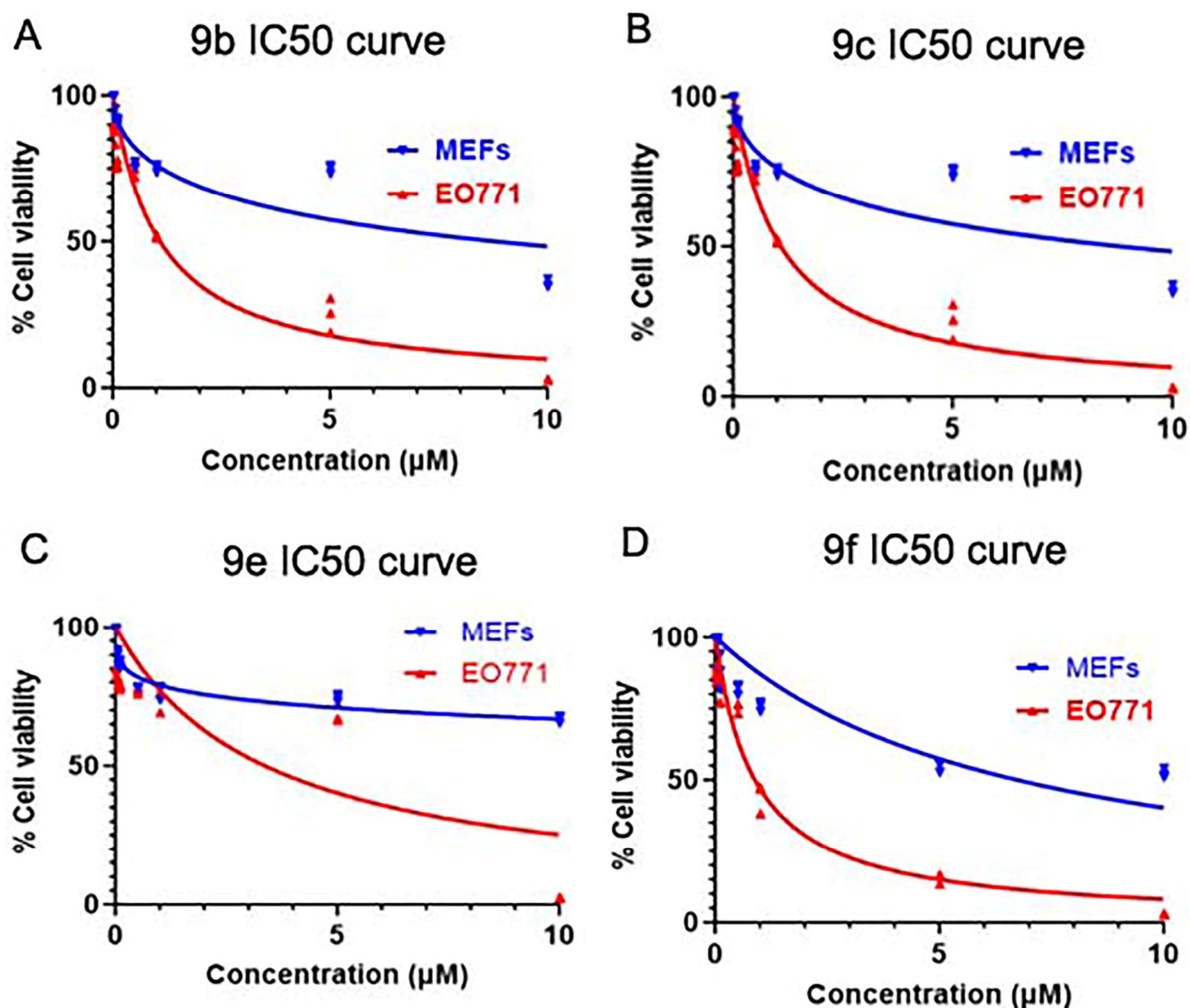


Figure 2. IC₅₀ curves of **9b**, **9c**, **9e** and **9f** were depicted in (A–D) respectively. The blue lines show the curves of the MEFs (non-cancerous cells). The red lines show the curves of the EO771 cells (mouse breast cancer cells).

3.4. Histological Analysis of the Tumors

The histology of the tumors revealed that all treatments affected both the proliferation of the cancer cells and their overall survival. Representative pictures of the Ki67 staining are depicted in Figure 4A. The proliferation index, measured by Ki67 immunohistochemistry (Figure 4B), showed that the control tumors had increased proliferation in contrast to the treated tumors (76.74% control vs. 41.95% **9b**, 43.47% **9c** and 41.08% **9e**). The reduced proliferation rates of all treated groups were statistically significant when compared to the untreated controls ($p = 1.23 \times 10^{-12}$, $p = 3.3 \times 10^{-12}$ and $p = 1.53 \times 10^{-13}$ for **9b**, **9c** and **9e** respectively).

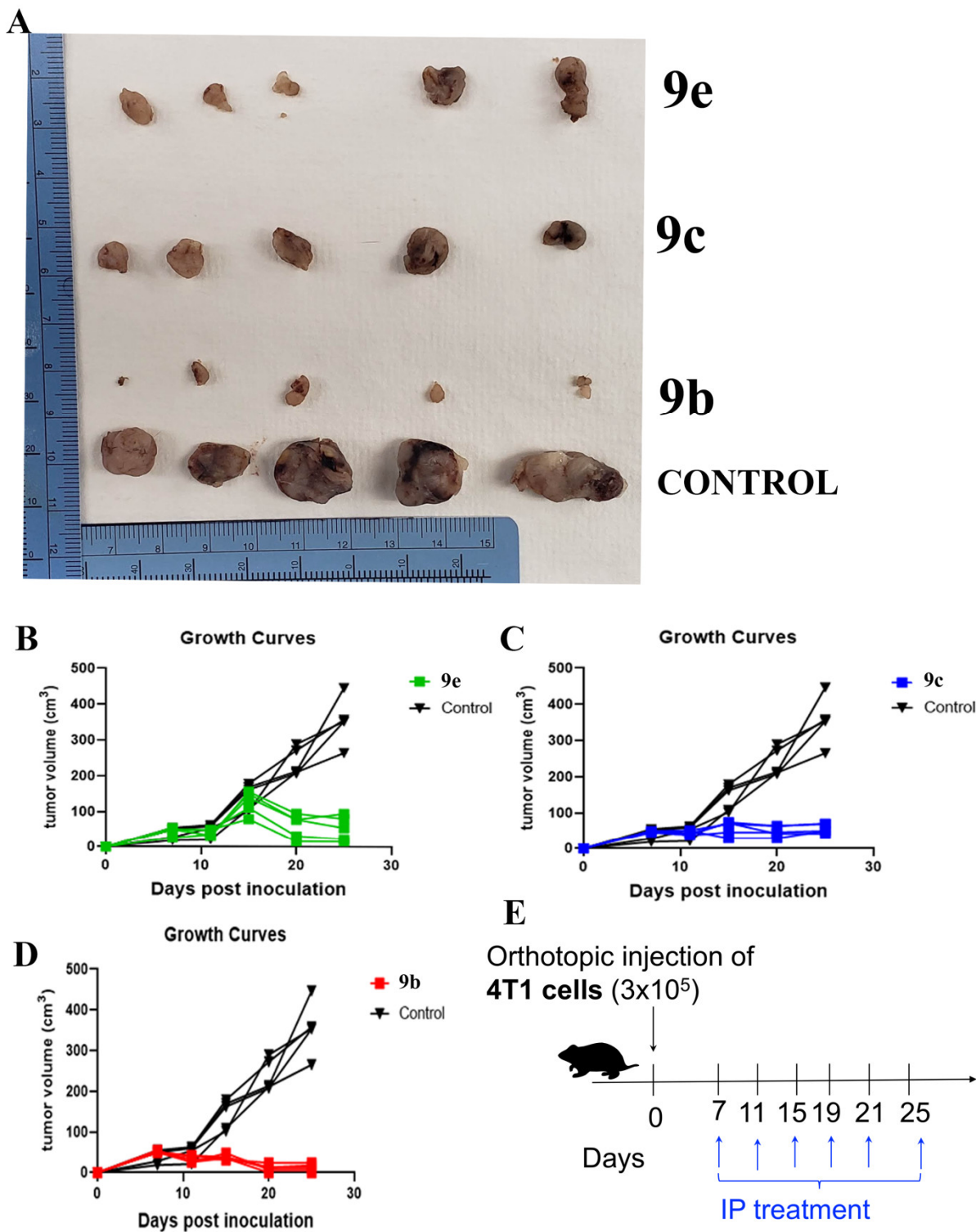


Figure 3. Efficacy of the **9e**, **9c** and **9b** in vivo. **(A)** Representative images of excised tumors. Lower panel control group, upper panels therapeutic groups. **(B)** Growth curves of **9e** (green) in comparison to the control (black). **(C)** Growth curves of **9c** (blue) in comparison to the control (black). **(D)** Growth curves of **9b** (red) in comparison to the control (black). **(E)** Treatment schedule. The in vivo experiments were performed three times with similar results; here we present representative images and growth curves from one experiment.

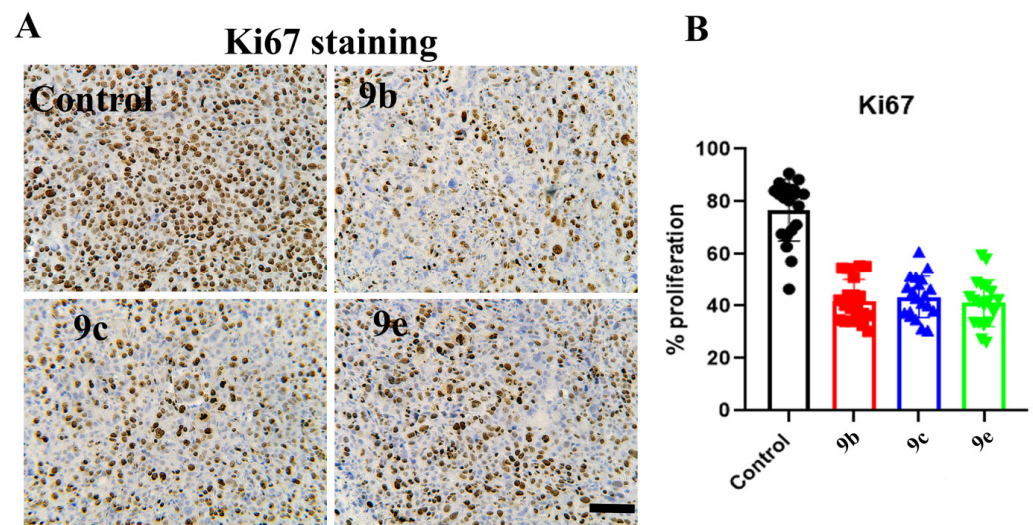


Figure 4. Panel (A) shows representative IHC images of Ki67 staining of control and treated tumors. In (B), the actual percentages of Ki67 per field were calculated. Scale bar 300 μ m. To determine proliferation indices, Ki67-positive and Ki67-negative cells were counted using ImageJ software (US National Institutes of Health) in 8–10 representative fields from each sample. All the samples were included in the analysis.

We next decided to analyze the apoptotic rate of cancer cells by using cleaved caspase-3 (Figure 5). For that purpose, we evaluated the staining in the periphery of the tumors rather than the staining on the central necrotic part. (Figure 5A). We observed an increase of the apoptotic cells in all the treated groups. The cleaved caspase-3 staining revealed a significant increase of the apoptotic cells ($p = 1.32 \times 10^{-5}$, $p = 0.03$, $p = 0.002$) in **9b**, **9c**, and **9e**, respectively. The mean percentages of apoptosis were 6.1% for the controls, 9.9% for **9b** treated, 7.68% for **9c**, and 8.37% for **9e** respectively. Most importantly, the **9b** treated tumors showed statistically significant increase in apoptosis in comparison to the other treated groups ($p = 0.009$ with **9c** and $p = 0.049$ with **9e**), which is also in line with our in vitro experiments.

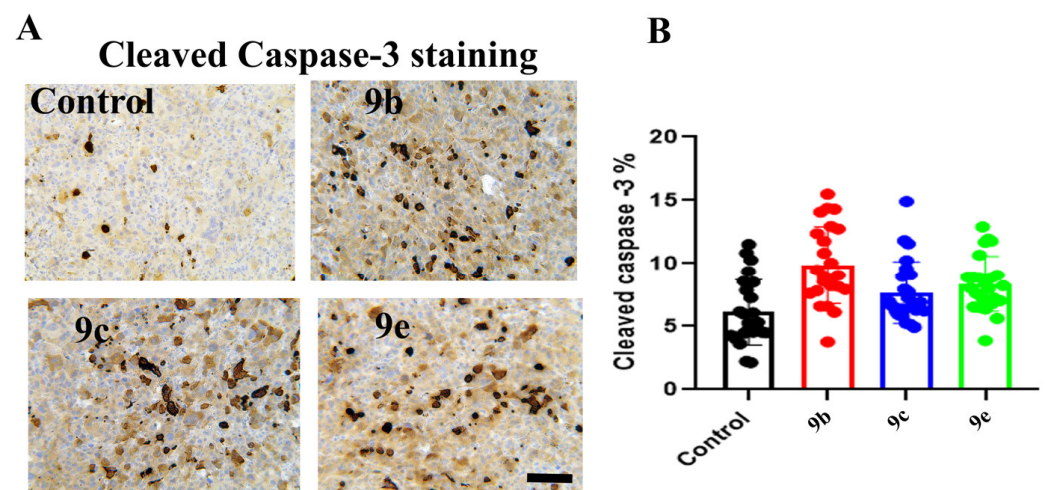


Figure 5. Panel (A) shows representative IHC images of cleaved caspase-3 staining of control and treated tumors. In (B), the actual percentages of cleaved caspase-3 per field were calculated. Scale bar 300 μ m. To determine apoptotic cells, cleaved caspase-3 positive and negative cells were counted using ImageJ software (US National Institutes of Health) in 8–10 representative fields from each sample. All the samples were included in the analysis.

4. Conclusions

In this work, a number of substituted pyrazolo[3,4-*b*]pyridines were prepared and tested for their antiproliferative activity. We decided not to alter the nature of the substituent in positions 1 and 6 of the scaffold; thus, we inserted 1-phenyl or 1-(3-fluorophenyl) group together with 6-phenylamino group in all target compounds. In total, we used a variety of 4-substituents and have studied their impact on the biological activity. Interestingly, the *in vitro* evaluation revealed that only 4-alkylaminoethoxy derivatives possessed strong cytotoxicity against the four cancer cell lines tested in the low μM range, while the normal cell line (normal mouse embryonic fibroblasts) remains practically unaffected. This finding prompted us to study the *in vivo* efficacy of the three most active analogues in a mouse breast cancer model. All compounds, and more profoundly, the 4-(4-methylpiperazin-1-yl)ethoxy derivative **9b**, presented a strong inhibition of tumor growth and induced apoptosis. It should be noted that these compounds do not show systemic toxicity and did not interfere with the immune system of the animals. More comprehensive structure–activity relationships, e.g., the necessity of the 1-phenyl (or fluorophenyl) substituent, as well as of the 6-phenylamino group, is currently under active investigation in our laboratories, with the aim of assisting in structure optimization and elucidating the molecular mode of action of this class of compounds.

Supplementary Materials: The following supporting information can be downloaded at: <https://www.mdpi.com/article/10.3390/pharmaceutics15030787/s1>, Certain synthetic procedures for intermediate compounds and spectroscopic data for all target compounds are provided.

Author Contributions: Conceptualization: N.P., P.M., N.L. and D.S.; Synthesis, purification and characterization of compounds: M.G. and N.L.; *in vitro* cytotoxicity experiments against PC-3 and HCT116 cells: K.G. and R.T.; histology experiments: E.D. and S.B.; *in vitro* (EO771, KPC, MEF cells), *in vivo* experiments: L.-E.G. and D.S.; formal analysis: M.G., K.G., N.L., S.B., L.-E.G. and E.D.; data curation: S.B., R.T., N.P., P.M., N.L. and D.S.; writing—original draft preparation, R.T., N.P., P.M., N.L. and D.S.; writing—review and editing, N.P., P.M. and D.S.; supervision, R.T., N.L. and D.S.; project administration, P.M. All authors have read and agreed to the published version of the manuscript.

Funding: This research received no external funding.

Institutional Review Board Statement: All studies were approved by the National Hellenic Research Foundation Animal Care and Use Committee. The study protocol was approved by the local ethics committee (Athens Prefecture Veterinarian Service; (431956/17-05-2022).

Informed Consent Statement: No experiments involving human samples were performed.

Data Availability Statement: All data are available upon request.

Conflicts of Interest: The authors declare no conflict of interest.

References

1. Xing, Y.; Zuo, J.; Krogstad, P.; Jung, M.E. Synthesis and Structure–Activity relationship (SAR) studies of novel pyrazolopyridine derivatives as inhibitors of enterovirus replication. *J. Med. Chem.* **2018**, *61*, 1688–1703. [[CrossRef](#)]
2. Miranda, M.D.; Chaves, O.A.; Rosa, A.S.; Azevedo, A.R.; da Silva Pinheiro, L.C.; Soares, V.C.; Dias, S.S.G.; Abrantes, J.L.; Bernardino, A.M.R.; Paixão, I.C.P.; et al. The Role of Pyrazolopyridine Derivatives on Different Steps of Herpes Simplex Virus Type-1 *In Vitro* Replicative Cycle. *Int. J. Mol. Sci.* **2022**, *23*, 8135. [[CrossRef](#)]
3. Ali, T.E. Synthesis of some novel pyrazolo[3,4-*b*]pyridine and pyrazolo[3,4-*d*]pyrimidine derivatives bearing 5,6-diphenyl-1,2,4-triazine moiety as potential antimicrobial agents. *Eur. J. Med. Chem.* **2009**, *44*, 4385–4392. [[CrossRef](#)]
4. El-Gohary, N.S.; Gabra, M.T.; Shaaban, M.I. Synthesis, molecular modeling and biological evaluation of new pyrazolo[3,4-*b*]pyridine analogs as potential antimicrobial, anti-quorum-sensing and anticancer agents. *Bioorg. Chem.* **2019**, *89*, 102976. [[CrossRef](#)]
5. Guercio, G.; Castoldi, D.; Giubellina, N.; Lamonica, A.; Ribecai, A.; Stabile, P.; Westerduin, P.; Dams, R.; Nicoletti, A.; Rossi, S.; et al. Overall synthesis of GSK356278: Quick delivery of a PDE4 inhibitor using a fit-for-purpose approach. *Org. Process Res. Dev.* **2010**, *14*, 1153–1161. [[CrossRef](#)]

6. Cantini, N.; Khlebnikov, A.I.; Crocetti, L.; Schepetkin, I.A.; Floresta, G.; Guerrini, G.; Vergelli, C.; Bartolucci, G.; Quinn, M.T.; Giovannoni, M.P. Exploration of nitrogen heterocycle scaffolds for the development of potent human neutrophil elastase inhibitors. *Bioorg. Med. Chem.* **2021**, *29*, 115836. [[CrossRef](#)]
7. Manetti, F.; Schenone, S.; Bondavalli, F.; Brullo, C.; Bruno, O.; Ranise, A.; Mosti, L.; Menozzi, G.; Fossa, P.; Trincavelli, M.L.; et al. Synthesis and 3D QSAR of new pyrazolo[3,4-*b*]pyridines: Potent and selective inhibitors of A1 adenosine receptors. *J. Med. Chem.* **2005**, *48*, 7172–7185. [[CrossRef](#)]
8. Atobe, M.; Naganuma, K.; Kawanishi, M.; Hayashi, T.; Suzuki, H.; Nishida, M.; Arai, H. Discovery of a novel 2-(1*H*-pyrazolo[3,4-*b*]pyridin-1-yl)thiazole derivative as an EP1 receptor antagonist and in vivo studies in a bone fracture model. *Bioorg. Med. Chem. Lett.* **2018**, *28*, 2408–2412. [[CrossRef](#)] [[PubMed](#)]
9. Eissa, I.H.; El-Naggar, A.M.; El-Hashash, M.A. Design, synthesis, molecular modeling and biological evaluation of novel 1*H*-pyrazolo[3,4-*b*]pyridine derivatives as potential anticancer agents. *Bioorg. Chem.* **2016**, *67*, 43–56. [[CrossRef](#)]
10. Atukuri, D. Pyrazolopyridine: An efficient pharmacophore in recent drug design and development. *Chem. Biol. Drug Des.* **2022**, *100*, 376–388. [[CrossRef](#)]
11. Barghash, R.F.; Eldehna, W.M.; Kovalová, M.; Vojáčková, V.; Kryštof, V.; Abdel-Aziz, H.A. One-pot three-component synthesis of novel pyrazolo[3,4-*b*]pyridines as potent antileukemic agents. *Eur. J. Med. Chem.* **2022**, *227*, 113952. [[CrossRef](#)] [[PubMed](#)]
12. Hao, S.-Y.; Qi, Z.-Y.; Wang, S.; Wang, X.-R.; Chen, S.-W. Synthesis and bioevaluation of *N*-(3,4,5-trimethoxyphenyl)-1*H*-pyrazolo[3,4-*b*]pyridin-3-amines as tubulin polymerization inhibitors with anti-angiogenic effects. *Bioorg. Med. Chem.* **2021**, *31*, 115985. [[CrossRef](#)]
13. Hassan, G.S.; Georgey, H.H.; Mohammed, E.Z.; George, R.F.; Mahmoud, W.R.; Omar, F.A. Mechanistic selectivity investigation and 2D-QSAR study of some new antiproliferative pyrazoles and pyrazolopyridines as potential CDK2 Inhibitors. *Eur. J. Med. Chem.* **2021**, *218*, 113389. [[CrossRef](#)] [[PubMed](#)]
14. Li, Y.; Cheng, H.; Zhang, Z.; Zhuang, X.; Luo, J.; Long, H.; Zhou, Y.; Xu, Y.R.; Taghipoura, R.; Li, D.; et al. *N*-(3-Ethynyl-2,4-difluorophenyl)sulfonamide derivatives as selective raf inhibitors. *ACS Med. Chem. Lett.* **2015**, *6*, 543–547. [[CrossRef](#)]
15. Liu, N.; Wang, Y.; Huang, G.; Ji, C.; Fan, W.; Li, H.; Cheng, Y.; Tian, H. Design, synthesis and biological evaluation of 1*H*-pyrrolo[2,3-*b*]pyridine and 1*H*-pyrazolo[3,4-*b*]pyridine derivatives as c-Met inhibitors. *Bioorg. Chem.* **2016**, *65*, 146–158. [[CrossRef](#)]
16. Argyros, O.; Lougiakis, N.; Kouvari, E.; Papafotika, A.; Raptopoulou, C.P.; Psycharis, V.; Christoforidis, S.; Pouli, N.; Marakos, P.; Tamvakopoulos, C. Design and Synthesis of Novel 7-Aminosubstituted pyrido[2,3-*b*]pyrazines Exhibiting Anti-breast Cancer Activity. *Eur. J. Med. Chem.* **2017**, *126*, 954–968. [[CrossRef](#)]
17. Gavriil, E.-S.; Doukatas, A.; Karampelas, T.; Myriantopoulos, V.; Dimitrakis, S.; Mikros, E.; Marakos, P.; Tamvakopoulos, C.; Pouli, N. Design, Synthesis and Biological Evaluation of Novel Substituted Purine Isosters as EGFR kinase inhibitors, with promising pharmacokinetic profile and in vivo efficacy. *Eur. J. Med. Chem.* **2019**, *176*, 393–409. [[CrossRef](#)] [[PubMed](#)]
18. Michailidou, M.; Giannouli, V.; Kotsikoris, V.; Papadodima, O.; Kontogianni, G.; Kostakis, I.K.; Lougiakis, N.; Chatziioannou, A.; Kollis, F.N.; Marakos, P.; et al. Novel pyrazolopyridine derivatives as potential angiogenesis inhibitors: Synthesis, biological evaluation and transcriptome-based mechanistic analysis. *Eur. J. Med. Chem.* **2016**, *121*, 143–157. [[CrossRef](#)]
19. Papastathopoulos, A.; Lougiakis, N.; Kostakis, I.K.; Marakos, P.; Pouli, N.; Pratsinis, H.; Kletsas, D. New bioactive 5-arylcarboximidamidopyrazolo[3,4-*c*]pyridines: Synthesis, cytotoxic activity, mechanistic investigation and structure-activity relationships. *Eur. J. Med. Chem.* **2021**, *218*, 113387. [[CrossRef](#)]
20. Lynch, B.M.; Khan, M.A.; Teo, H.C.; Pedroti, F. Pyrazolo[3,4-*b*]pyridines: Syntheses, reactions, and nuclear magnetic resonance spectra. *Can. J. Chem.* **1988**, *66*, 420–428. [[CrossRef](#)]
21. Stellas, D.; Szabolcs, M.; Koul, S.; Li, Z.; Polyzos, A.; Anagnostopoulos, C.; Cournia, Z.; Tamvakopoulos, C.; Klinakis, A.; Efstratiadis, A. Therapeutic Effects of an Anti-Myc Drug on Mouse Pancreatic Cancer. *J. Natl. Cancer Inst.* **2014**, *106*, dju320. [[CrossRef](#)] [[PubMed](#)]
22. Vistica, D.T.; Skehan, P.; Scudiero, D.; Monks, A.; Pittman, A.; Boyd, M.R. Tetrazolium-based assays for cellular viability: A critical examination of selected parameters affecting formazan production. *Cancer Res.* **1991**, *51*, 2515–2520. [[PubMed](#)]
23. Pippa, N.; Naziris, N.; Stellas, D.; Massala, C.; Zouliati, K.; Pispas, S.; Demetzos, C.; Forys, A.; Marcinkowski, A.; Trzebicka, B. PEO-*b*-PCL grafted niosomes: The cooperativity of amphiphilic components and their properties in vitro and in vivo. *Colloids Surf. B Biointerfaces* **2019**, *177*, 338–345. [[CrossRef](#)] [[PubMed](#)]
24. Smolobochkin, A.V.; Gazizov, A.S.; Garifzyanov, A.R.; Burirov, A.R.; Pudovika, M.A. Methods for the synthesis of 1*H*-pyrazolo[3,4-*b*]pyridine derivatives. *Russ. Chem. Bull.* **2022**, *71*, 878–884. [[CrossRef](#)]
25. Quiroga, J.; Hormanza, A.; Insuasty, B. Reaction of 5-amino-1-aryl-3-methylpyrazoles with benzylidene derivatives of meldrum's acid: Synthesis and characterization of pyrazolo[3,4-*b*]pyridinones. *J. Heterocycl. Chem.* **1998**, *35*, 409–412. [[CrossRef](#)]
26. Somakala, K.; Tariq, S.; Amir, M. Synthesis, evaluation and docking of novel pyrazolopyrimidines as potent p38 α MAP kinase inhibitors with improved anti-inflammatory, ulcerogenic and TNF- α inhibitory properties. *Bioorg. Chem.* **2019**, *87*, 550–559. [[CrossRef](#)]
27. Harden, F.A.; Quinn, R.J.; Scammells, P.J. Synthesis and adenosine receptor affinity of a series of pyrazolo[3,4-*d*]pyrimidine analogs of 1-methylisoguanosine. *J. Med. Chem.* **1991**, *34*, 2892–2898. [[CrossRef](#)]

28. Chen, H.; Wang, B.; Li, P.; Yan, H.; Li, G.; Huang, H.; Lu, Y. The optimization and characterization of functionalized sulfonamides derived from sulfaphenazole against Mycobacterium tuberculosis with reduced CYP 2C9 inhibition. *Bioorg. Med. Chem. Lett.* **2021**, *40*, 127924. [[CrossRef](#)]
29. Pirali, T.; Ciralo, E.; Aprile, S.; Massarotti, A.; Berndt, A.; Griglio, A.; Serafini, M.; Mercalli, V.; Landoni, C.; Campa, C.C.; et al. Tron Identification of a Potent Phosphoinositide 3-Kinase Pan Inhibitor Displaying a Strategic Carboxylic Acid Group and Development of Its Prodrugs. *ChemMedChem* **2017**, *12*, 1542–1554. [[CrossRef](#)]

Disclaimer/Publisher's Note: The statements, opinions and data contained in all publications are solely those of the individual author(s) and contributor(s) and not of MDPI and/or the editor(s). MDPI and/or the editor(s) disclaim responsibility for any injury to people or property resulting from any ideas, methods, instructions or products referred to in the content.